

# Supporting Information

## N-Doped CoSb@C Nanofibers as Self-Supporting Anode for High-Performance K-Ion and Na-Ion Batteries

*Jun Han<sup>a,b</sup>, Kunjie Zhu<sup>b</sup>, Pei Liu<sup>b</sup>, Yuchang Si<sup>c\*</sup>, Yujun Chai<sup>a\*</sup>, Lifang Jiao<sup>b\*†</sup>*

*a. College of Chemistry and Materials Science, Hebei Normal University,  
Shijiazhuang 050020, China*

*b. Key Laboratory of Advanced Energy Materials Chemistry (Ministry of  
Education), Renewable Energy Conversion and Storage Center, College of  
Chemistry, Nankai University, Tianjin 300071, China*

*c. Logistics University of People's Armed Police Force, China*

E-mail: [jiaolf@nankai.edu.cn](mailto:jiaolf@nankai.edu.cn). (L.J.)

\*Corresponding author

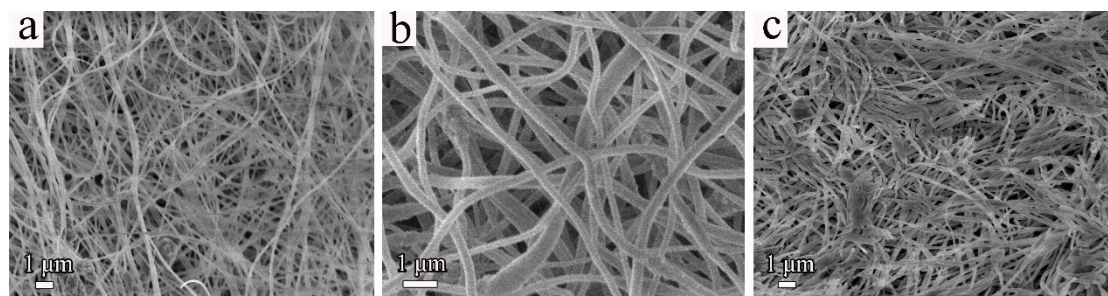


**Figure S1.** The SEM morphology of as-collected fibers with different mass of PAN.

a) 0.4g b) 0.6g c) 0.8g

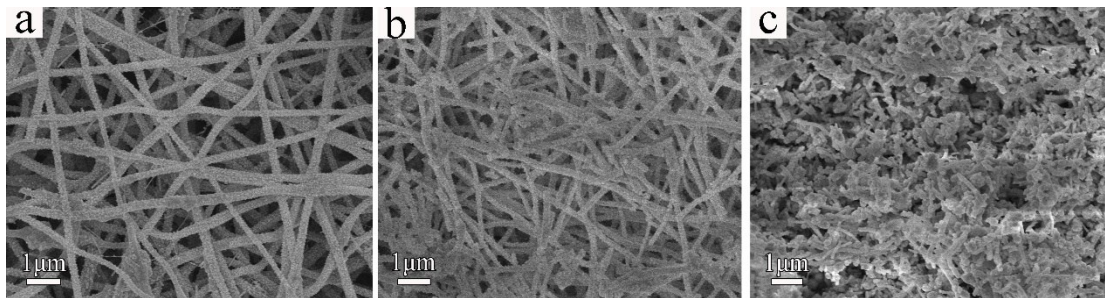


**Figure S2.** The SEM morphology of fibers with different carbonized temperature.

a) 600°C b) 700°C c) 800°C

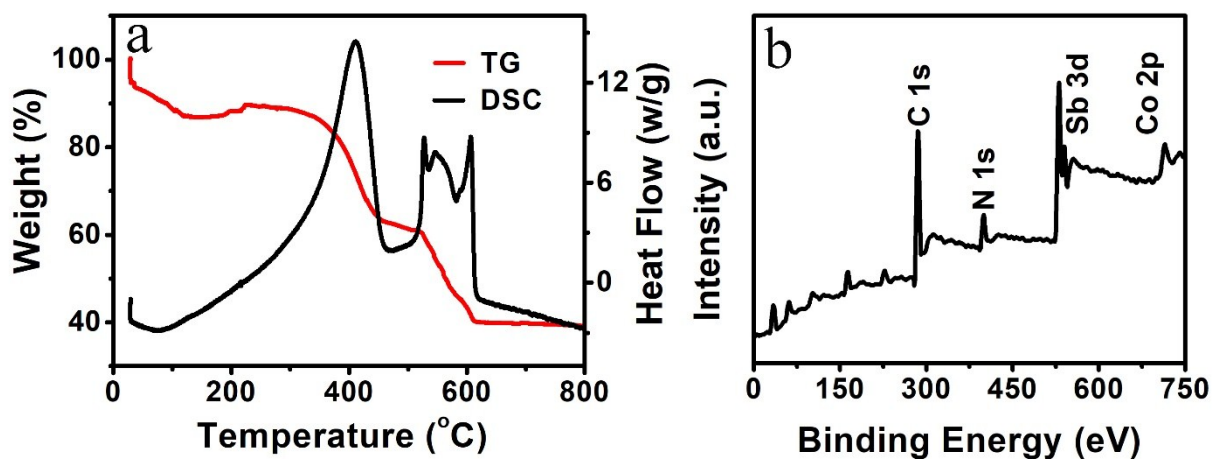


**Figure S3.** a) TG-DSC curves in the air environment with a heating rate of 5 °C min<sup>-1</sup> b) XPS spectrum of CoSb@C nanofibers.

As shown in Fig. S3a, the weight loss ( $\leq 200$  °C) was due to the elimination of absorbed water. The weight decline (300 °C ~ 400 °C) was caused by the combustion of carbon. The weight change between 500 °C to 600 °C could be caused by the reaction of metallic volatilization and oxidation.

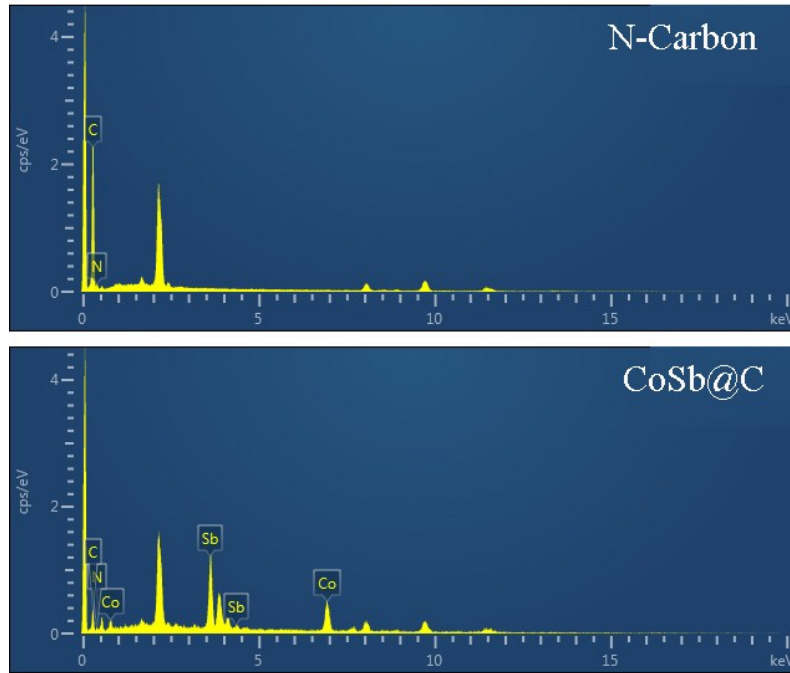


**Fig. S4.** EDS elements analysis of carbon and CoSb@C nanofibers.

Sample	N-Carbon		N-CoSb@C			
Elements	C	N	C	N	Co	Sb
Content (at%)	75.35	24.65	56.12	13.37	15.79	14.72
Content (wt%)	72.37	27.62	18.77	5.21	25.96	50.06

**Table S1.** Element content of carbon and CoSb@C nanofibers derived from EDS.

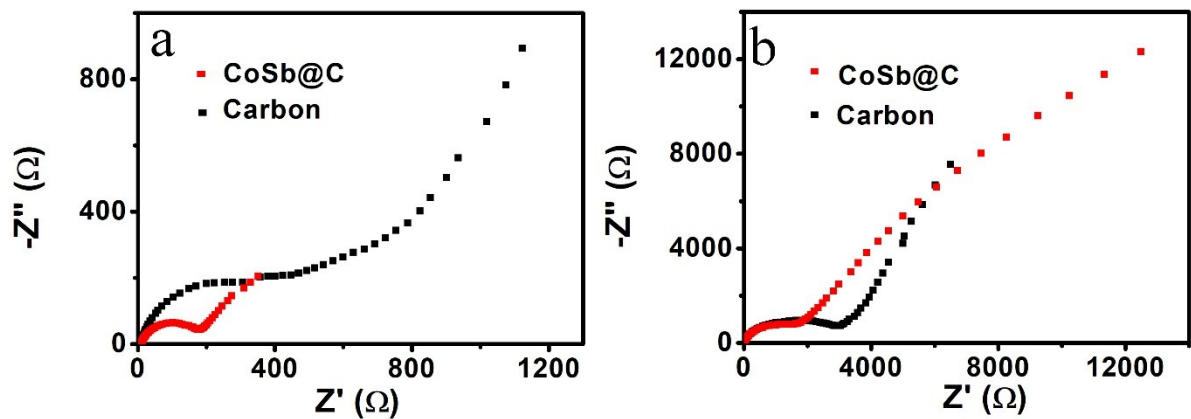


**Figure S5.** Nyquist plots of CoSb@C nanofibers. a) SIBs and b) PIBs.

The doping of nitrogen elements can create defect sites to optimize the electronic configuration of carbon materials (the CoSb@C nanofibers and carbon nanofibers), improving the electronic conductivity. However, the charge-transfer resistance of the CoSb@C nanofibers is relatively diminutive, corroborating the faster Na<sup>+</sup>/K<sup>+</sup> migration rate, which is mainly caused by the unique structure and CoSb alloy.

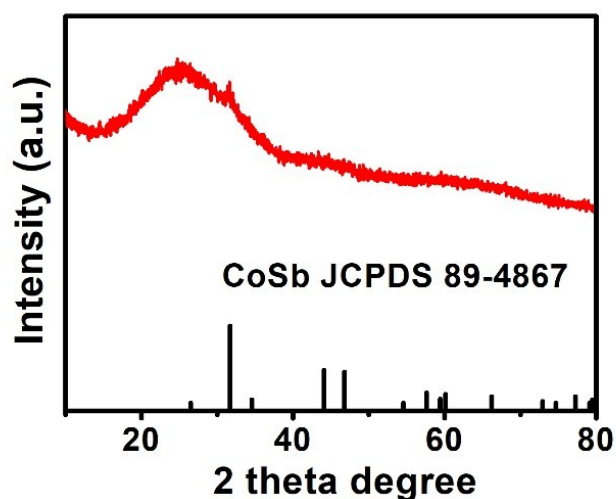


**Figure S6.** XRD patterns of CoSb@C nanofibers over 100 cycles in PIBs.

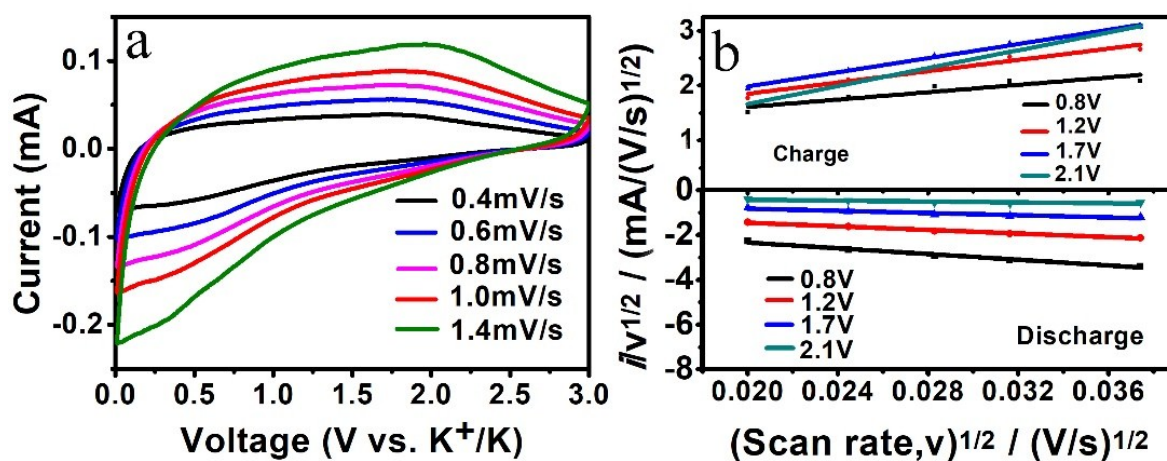


**Figure S7.** a) The different sweep-rate CVs behavior (0.01-3.0 V), b) Plots of  $i/v^{1/2}$  vs.  $v^{1/2}$  used for calculating constants  $k_1$  and  $k_2$  at different potentials of CoSb@C nanofibers in PIBs.

Plots of  $i/v^{1/2}$  vs.  $v^{1/2}$  at different potentials can be used for calculating constants  $k_1$  (slope) and  $k_2$  (intercept) of CoSb@C nanofibers in PIBs. When the potential is settled, the current ( $i$ ) is composed of pseudocapacitance-predominant process ( $k_1v$ ) and diffusion process ( $k_2v^{1/2}$ ). From this procedure, the quantified evaluation can be applied to determine the extent of two kinetics process.

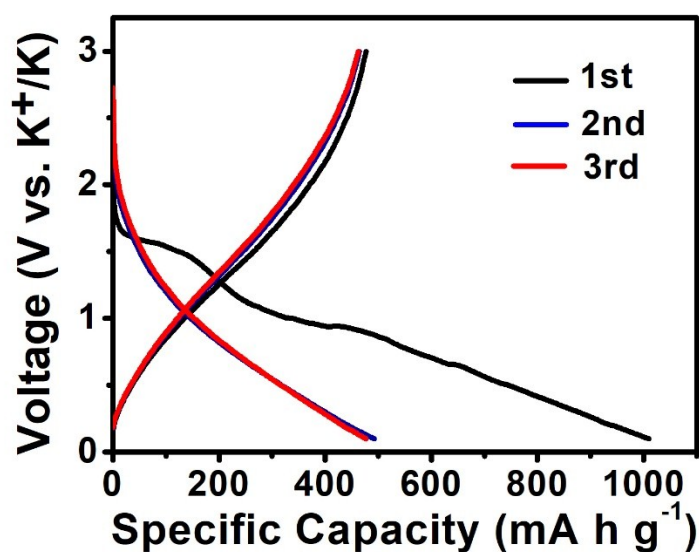


**Figure S8.** Galvanostatic charge/discharge curves (100 mA g<sup>-1</sup>, 0.01 V-3.0 V) of PIBs.

As is well-known, the obvious plateaus are a typical feature of diffusion process, and the more moderate and continuous operation voltage with sloping platforms is the feature of the pseudocapacitive behavior in the galvanostatic charge/discharge curves.

Then, the galvanostatic charge/discharge curves (Figure S8) with non-typic platforms (100 mA g<sup>-1</sup>, 0.01 V-3.0 V) indicate the co-existence of the pseudocapacitive behavior and diffusion process.

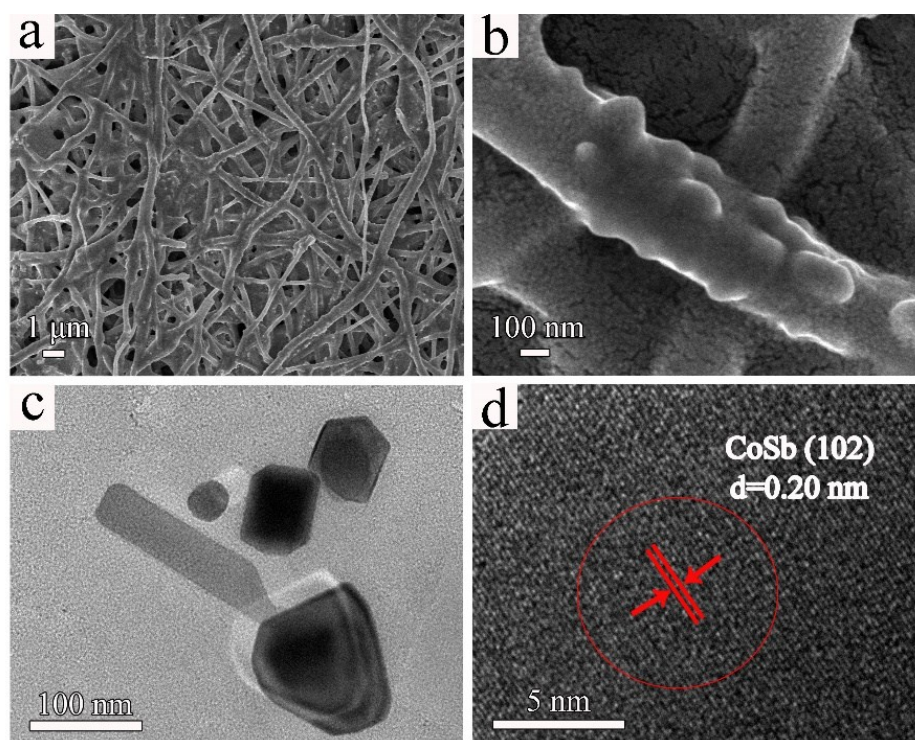


**Figure S9.** a) SEM, b) High-resolution SEM, c) TEM, d) HRTEM images of CoSb@C nanofibers over 100 cycles in SIBs.

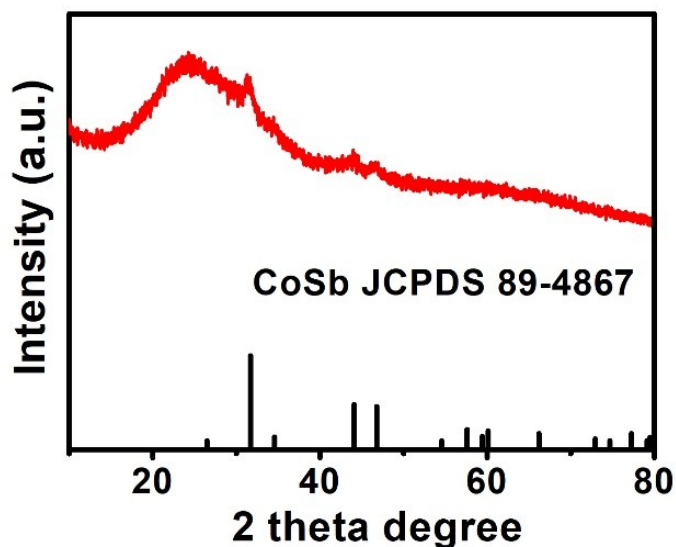


Figure S10. XRD patterns of CoSb@C nanofibers over 100 cycles in SIBs.

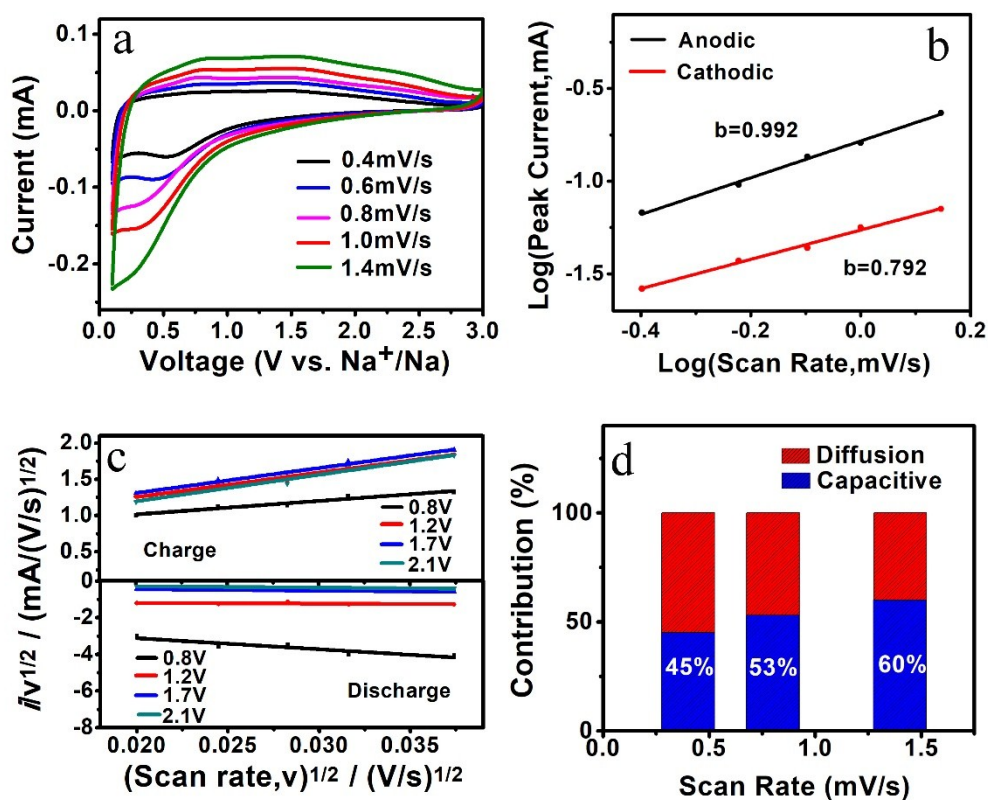
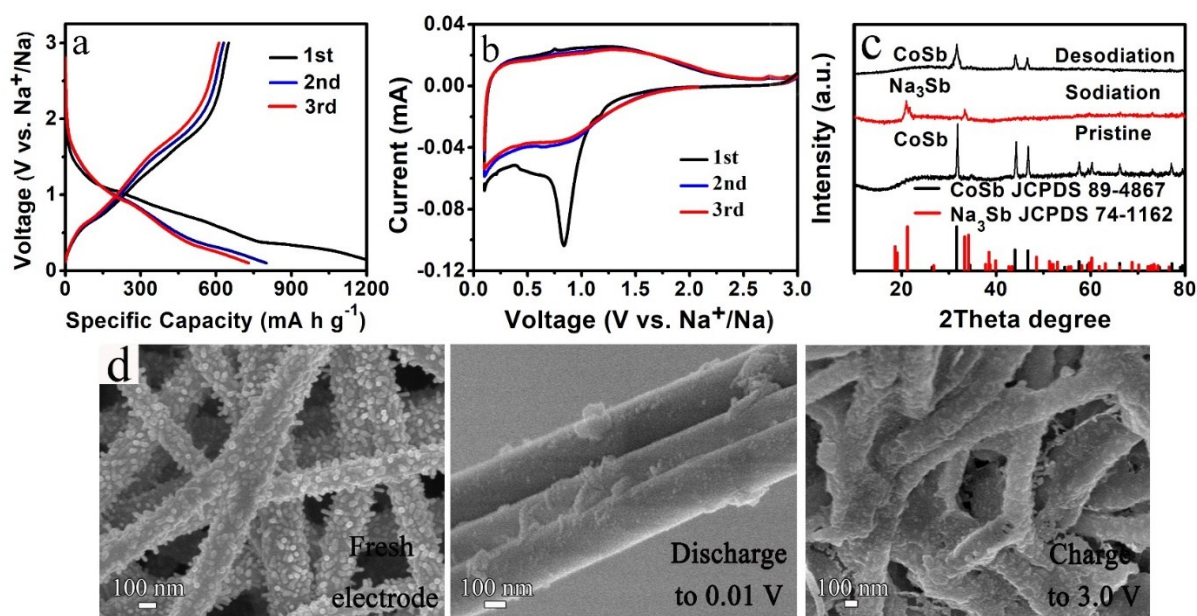


Figure S11. a) The different sweep-rate CVs behavior (0.01-3.0 V), b) The value of  $b$ , c) Plots of  $i/v^{1/2}$  vs.  $v^{1/2}$  used for calculating constants  $k_1$  and  $k_2$  at different potentials and d) Capacitive contributions with different scan rates of CoSb@C

nanofibers in SIBs.

The reaction kinetics of CoSb@C nanofibers has been inspected by different sweep-rate cyclic voltammograms (CVs) in Figure S11a. The value of  $b$  in Figure S11b shows that reaction kinetics of CoSb@C nanofibers is controlled by pseudocapacitance process and diffusion process (alloying). Figure S11d displays the capacitive contributions of 45%, 53%, 60% at the scan rates of 0.4, 0.8, 1.4  $\text{mV s}^{-1}$ , respectively, which indicates that the pseudocapacitance accelerate the rate property.



**Figure S12.** a) Galvanostatic charge/discharge curves ( $100 \text{ mA g}^{-1}$ , 0.01 V-3.0 V), b) the CV behavior ( $0.01\text{-}3.0 \text{ V}$ ,  $0.1 \text{ mV s}^{-1}$ ) of CoSb@C nanofibers, c) XRD patterns of 1<sup>st</sup> charge/discharge products, d) SEM images of CoSb@C nanofibers in first-cycle process in SIBs.

Figure S12a reveals the galvanostatic charge/discharge curves ( $100 \text{ mA g}^{-1}$ , 0.01 V-3.0 V). In Figure S12b, the cyclic CV behavior ( $0.01\text{-}3 \text{ V}$ ,  $0.1 \text{ mV s}^{-1}$ ) of CoSb@C nanofibers confirms its glorious cyclic performance once more. In the initial discharge

process, three peaks can be observed at 0.21 V, 0.43 V and 0.82 V, which are caused by the formation of  $\text{Na}_x\text{Sb}$  ( $x \leq 3$ ) alloy and SEI layers. The following peaks from 0.7 V-1.0 V correspond with the formation of  $\text{Na}_x\text{Sb}$  and then  $\text{Na}_3\text{Sb}$  alloy.

In the charge process, a broad peak around 0.75V is attributed to the desodiation of  $\text{Na}_3\text{Sb}$  alloy, and the peak at 2.73 V is caused by side reactions of electrolyte.<sup>1,2</sup> The progress can be tested by XRD and SEM in Figure S12c-d.<sup>3</sup> In the end, the reactions are as following:



<b>Anode materials</b>	<b>Synthetic method</b>	<b>Electrochemical performance</b>	<b>Ref.</b>
3D NP-Sb	vacuum distillation method	318 mAh g <sup>-1</sup> (50 cycles, 100 mA g <sup>-1</sup> , PIBs)	[7]
Sb@CSN	electrospray assisted method	551 mAh g <sup>-1</sup> (100 cycles, 100 mA g <sup>-1</sup> , PIBs)	[9]
CoSb@C nanofiber	electrospinning	449 mAh g <sup>-1</sup> (160 cycles, 100 mA g <sup>-1</sup> , PIBs)	This Work
Sb-C nanofiber	electrospinning	495 mAh g <sup>-1</sup> (400 cycles, 200 mA g <sup>-1</sup> , SIBs)	[15]
Sb@(N, S-C)	annealing the mixture solution	621 mAh g <sup>-1</sup> (150 cycles, 100 mA g <sup>-1</sup> , SIBs)	[37]
Sb-C	sol-gel method	305 mAh g <sup>-1</sup> (60 cycles, 50 mA g <sup>-1</sup> , SIBs)	[43]
SnSb NCs	surfactant-free synthesis	560 mAh g <sup>-1</sup> (100 cycles, 200 mA g <sup>-1</sup> , SIBs)	[22]
SnSb/NPCNWs	electrospinning	180 mAh g <sup>-1</sup> (10000 cycles, 2000 mA g <sup>-1</sup> , SIBs)	[36]
Fe-Sb alloy	melt-spinning process	466 mAh g <sup>-1</sup> (50 cycles, 80 mA g <sup>-1</sup> , SIBs)	[27]
Bi <sub>0.57</sub> Sb <sub>0.43</sub> -C	mechanical milling method	410 mAh g <sup>-1</sup> (300 cycles, 200 mA g <sup>-1</sup> , SIBs)	[28]
CoSb@C	electrospinning	708 mAh g <sup>-1</sup> (200 cycles, 200 mA g <sup>-1</sup> , SIBs)	This Work

Table S2. Electrochemical performance of Sb-based materials for PIBs and SIBs

**References:**

1. X. Zhou, Y. Zhong, M. Yang, M. Hu, J. Wei and Z. Zhou, *Chem. Commun.*, 2014, **50**, 12888-12891.
2. B. Selvaraj, S.-S. Huang, C.-E. Wu, Y.-H. Lin, C.-C. Wang, Y.-F. Song, M.-L. Lu, H.-S. Sheu and N.-L. Wu, *ACS Appl. Energy Mater.*, 2018, **1**, 2317-2325.
3. X. Zhang, P. Li, R. Zang, S. Wang, Y. Zhu, C. Li and G. Wang, *Chem Asian J*, 2017, **12**, 116-121